

# The $\gamma\gamma \rightarrow J/\psi J/\psi$ reaction and the $J/\psi J/\psi$ pair production in exclusive ultraperipheral ultrarelativistic heavy ion collisions

Sergey Baranov,<sup>1,\*</sup> Anna Cisek,<sup>2,†</sup> Mariola Klusek-Gawenda,<sup>2,‡</sup>  
Wolfgang Schäfer,<sup>2,§</sup> and Antoni Szczurek<sup>2,3,¶</sup>

<sup>1</sup>*P.N. Lebedev Institute of Physics, 53 Lenin Avenue, Moscow 119991, Russia*

<sup>2</sup>*Institute of Nuclear Physics PAN, PL-31-342 Cracow, Poland*

<sup>3</sup>*University of Rzeszów, PL-35-959 Rzeszów, Poland*

(Dated: October 15, 2018)

## Abstract

We calculate the cross section for the  $\gamma\gamma \rightarrow J/\psi J/\psi$  process. Two mechanisms are considered: box (two-loop) diagrams of the order of  $O(\alpha_{em}^2 \alpha_s^2)$  and two-gluon exchange of the order of  $O(\alpha_{em}^2 \alpha_s^4)$ . The first mechanism is calculated in the heavy-quark non-relativistic approximation while the second case we also include the effects of quantum motion of quarks in the bound state. The box contribution dominates at energies close to the threshold ( $W < 15$  GeV) while the two-gluon mechanism takes over at  $W > 15$  GeV. Including the bound-state wave function effects for the two-gluon exchange mechanism gives a cross section 0.1 - 0.4 pb, substantially smaller than that in the non-relativistic limit (0.4 - 1.6 pb). We also find a strong infrared sensitivity which manifests itself in a rather strong dependence on the mass for the  $t$ -channel gluons. The elementary cross section is then used in the Equivalent Photon Approximation (EPA) in the impact parameter space to calculate the cross section for  $^{208}\text{Pb} + ^{208}\text{Pb} \rightarrow ^{208}\text{Pb} + J/\psi J/\psi + ^{208}\text{Pb}$  reaction. Distributions in rapidity of the  $J/\psi J/\psi$  pair and invariant mass of the pair are shown.

PACS numbers: 12.38.Bx, 13.85.Ni, 14.40.Pq

---

\*Electronic address: baranov@sci.lebedev.ru

†Electronic address: anna.cisek@ifj.edu.pl

‡Electronic address: mariola.klusek@ifj.edu.pl

§Electronic address: wolfgang.schafer@ifj.edu.pl

¶Electronic address: antoni.szczurek@ifj.edu.pl

## I. INTRODUCTION

The two-photon collisions is a natural place to study vector-meson pair production. Production of light vector mesons is rather of nonperturbative nature and therefore subjected to more phenomenological studies. Heavy vector meson production ( $J/\psi$  or  $\Upsilon$ ) is particularly interesting as here the pQCD degrees of freedom can be applied and hopefully reliable predictions can be obtained. It was realized quite early that in the high-energy limit the two-gluon exchange is the dominant reaction mechanism of two heavy vector meson production. The relevant amplitude was calculated first in the heavy-quark non-relativistic approximation in [1], and first estimates of the cross section were presented there. The impact factors of [1] were used next to estimate BFKL effects e.g. in [2, 3]. Some other estimates based on parametrizing dipole-dipole interaction were presented in [4]. Perhaps surprisingly, there is actually a substantial spread in the predictions shown in those works, they do not seem consistent one with each other and differ by almost two orders of magnitude. For a number of reasons, it seems that these previous evaluations are not very realistic in the intermediate energy range relevant to studies of the  $\gamma\gamma$  sub-process in nucleus-nucleus collisions.

Firstly, the process considered in the mentioned papers is not the lowest order of strong coupling constant. Formally lower-order processes of the box type were studied in [5]. In these calculation heavy-quark approximation was used in order to calculate the two-loop amplitudes. At high energies, these mechanisms correspond to the quark-antiquark exchanges in the crossed channels and will die out with increasing  $\gamma\gamma$  energies. The numerical predictions of [5] were however shown only at high (linear collider) energies ( $\sqrt{s} > 400$  GeV) where this mechanism is definitely not the dominant one.

Secondly, previous calculations of the two-gluon exchange mechanism were restricted to the extreme non-relativistic limit, and neglect the motion of heavy quarks in the bound state. Here, we shall calculate the two-gluon exchange contribution using for the first time for this process relativistic non-forward impact factors. Furthermore, by introducing a gluon mass, we investigate the infrared sensitivity of the amplitude, which turns out to be rather strong.

Therefore in the present work we wish to discuss both mechanisms simultaneously and discuss and identify the region of their dominance.

Finally we shall present realistic predictions for heavy ion collisions where the fluxes of quasi-real photons are very large. Here one may be able to study such processes in the near future.

## II. FORMALISM

In the present approach we include processes shown in Figs. 1, 2, 3. Now we shall discuss each of the mechanisms one by one.

### A. Box diagrams

At the leading order,  $\mathcal{O}(\alpha^2\alpha_s^2)$ , the sub-process  $\gamma + \gamma \rightarrow J/\psi + J/\psi$  is represented by the 20 "box" diagrams shown in Fig.1 The calculations are straightforward and follow the standard QCD rules and non-relativistic bound state formalism described in detail in Refs. [6]. As usual, the production amplitudes contain spin and color projection operators that

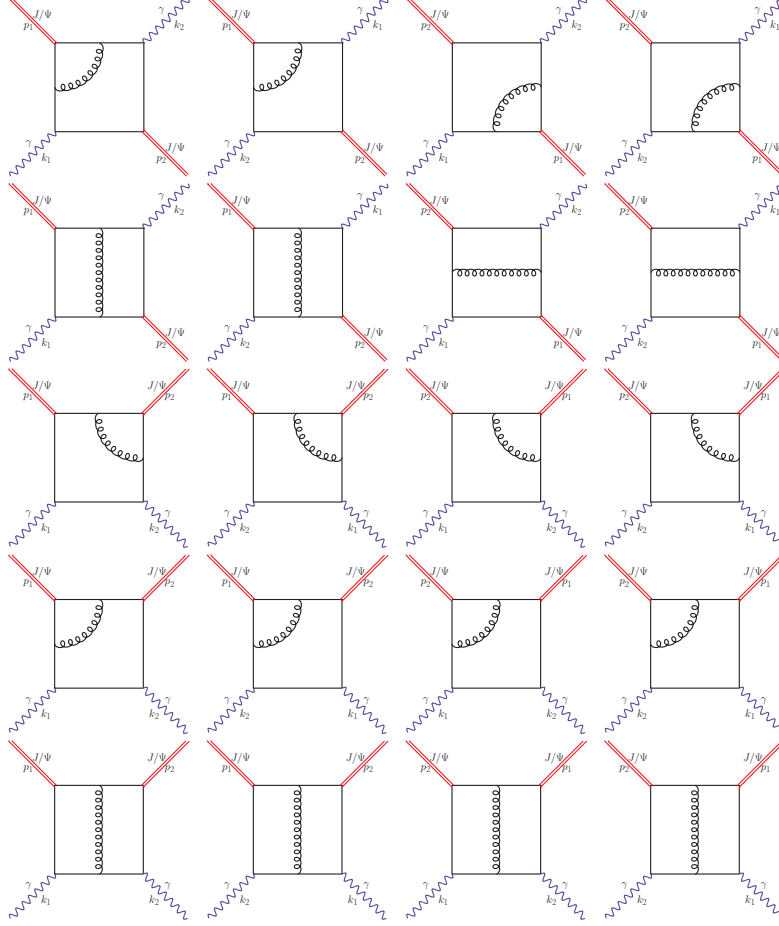


FIG. 1: The “box” diagrams for  $\gamma\gamma \rightarrow J/\psi J/\psi$  included in the present paper in the heavy-quark approximation.

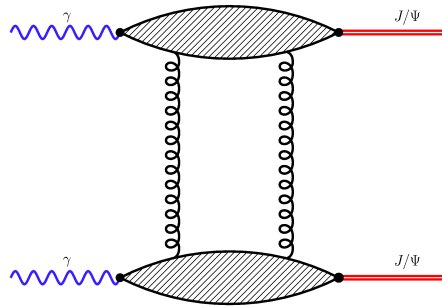


FIG. 2: Graphical representation of the two-gluon exchange mechanism for  $\gamma\gamma \rightarrow J/\psi J/\psi$ .

guarantee the proper quantum numbers of the final state mesons. The formation of the  $c\bar{c}$  bound states is determined by the  $J/\psi$  wave function at the origin of coordinate space,  $|\psi(0)|^2$ ; its value is known from the leptonic decay width:  $|\psi(0)|^2 = |\mathcal{R}(0)|^2/(4\pi) = 0.08 \text{ GeV}^3$  [7]. Only the color-singlet channels are taken into consideration in the present study.

Our calculation is identical to that of Ref. [5], with the only exception that we consider individual helicity amplitudes rather than the entire spin-averaged matrix element. The

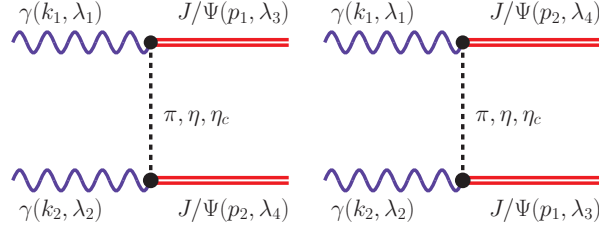


FIG. 3: Graphical representation of the meson exchange diagrams for  $\gamma\gamma \rightarrow J/\psi J/\psi$ .

polarization vectors of the initial photons and outgoing mesons are presented in our approach as explicit 4-vectors. For a particle moving along the  $z$ -axis,  $p^\mu = (0, 0, |p|, E)$ , the helicity eigenstate vectors have the form

$$\epsilon^\mu(\pm 1) = (\pm 1, i, 0, 0)/\sqrt{2}, \quad \epsilon^\mu(0) = (0, 0, E, |\vec{p}|)/m.$$

The evaluation of the Feynman diagrams has been done using the algebraic manipulation system FORM [8]. We have checked that after performing numerical summation over all possible polarization states we arrive at the same result as the one given by Eq.(4) in Ref. [5].

In practical calculation we take leading-order formula for  $\alpha_s$  which is evaluated at  $\mu_r^2 = 4m_c^2$ .

## B. Two-gluon exchange

At sufficiently high energies, the box diagram contributions, which contain the fermion-antifermion exchange in the crossed channels die out, and the cross section will be dominated by diffractive mechanisms. The Feynman diagrams for the diffractive  $\gamma\gamma \rightarrow VV$  amplitude is depicted in Fig.2. Although it is formally of higher order in  $\alpha_s$  than the box mechanism, the crossed channel gluon exchanges do not die out with energy.

### 1. Relativistic approach

The altogether 16 diagrams of the type shown in Fig.2 can be lead to the amplitude, which can be cast into the impact-factor representation:

$$A(\gamma_{\lambda_1} \gamma_{\lambda_2} \rightarrow V_{\lambda_3} V_{\lambda_4}; s, t) = is \int d^2\kappa \frac{\mathcal{J}(\gamma_{\lambda_1} \rightarrow V_{\lambda_3}; \kappa, \mathbf{q}) \mathcal{J}(\gamma_{\lambda_2} \rightarrow V_{\lambda_4}; -\kappa, -\mathbf{q})}{[(\kappa + \mathbf{q}/2)^2 + \mu_G^2][(\kappa - \mathbf{q}/2)^2 + \mu_G^2]}. \quad (2.1)$$

Here  $\mathbf{q}$  is the transverse momentum transfer,  $t \approx -\mathbf{q}^2$ , and  $\mu_G$  is a gluon mass parameter. Notice, that the amplitude is finite at  $\mu_G \rightarrow 0$ , because the impact factors  $\mathcal{J}$  vanish for  $\kappa \rightarrow \pm \mathbf{q}/2$ . Graphical representation of the impact factors is shown in Fig.4.

The amplitude is normalized such, that differential cross section is given by

$$\frac{d\sigma(\gamma\gamma \rightarrow VV; s)}{dt} = \frac{1}{16\pi s^2} \frac{1}{4} \sum_{\lambda_i} \left| A(\gamma_{\lambda_1} \gamma_{\lambda_2} \rightarrow V_{\lambda_3} V_{\lambda_4}; s, t) \right|^2. \quad (2.2)$$

At small  $t$ , within the diffraction cone, the cross section is dominated by the  $s$ -channel helicity conserving amplitude. In this case, the explicit form of the impact factor is

$$\mathcal{J}(\gamma_\lambda \rightarrow V_\tau; \boldsymbol{\kappa}, \mathbf{q}) = \delta_{\lambda,\tau} \sqrt{N_c^2 - 1} \alpha_S e_Q \sqrt{4\pi\alpha_{em}} \int \frac{dz d^2\mathbf{k}}{z(1-z)(2\pi)^3} \psi_V(z, \mathbf{k}) I(T, T), \quad (2.3)$$

where  $N_c = 3$  is the number of colors,  $e_Q$  is the charge of the heavy quark, and  $\psi_V(z, \mathbf{k})$  is the light-cone wave function of the vector meson. It depends on the light-cone-plus momentum fraction  $z$  carried by the quarks as well as on the quark transverse momentum  $\mathbf{k}$ . The spinorial structure of the  $V \rightarrow Q\bar{Q}$  vertex has been chosen such that it describes the  $S$ -wave bound state of quarks [9], so that

$$I(T, T) = m_Q^2 \Phi_2 + \left[ z^2 + (1-z)^2 \right] (\mathbf{k}\Phi_1) + \frac{m_Q}{M + 2m_Q} \left[ \mathbf{k}^2 \Phi_2 - (2z-1)^2 (\mathbf{k}\Phi_1) \right]. \quad (2.4)$$

Here  $\Phi_1, \Phi_2$  are shorthand notations for the momentum structures, corresponding to the four relevant Feynman diagrams:

$$\begin{aligned} \Phi_2 &= -\frac{1}{(\mathbf{l} + \boldsymbol{\kappa})^2 + m_Q^2} - \frac{1}{(\mathbf{l} - \boldsymbol{\kappa})^2 + m_Q^2} + \frac{1}{(\mathbf{l} + \mathbf{q}/2)^2 + m_Q^2} + \frac{1}{(\mathbf{l} - \mathbf{q}/2)^2 + m_Q^2} \\ \Phi_1 &= -\frac{\mathbf{l} + \boldsymbol{\kappa}}{(\mathbf{l} + \boldsymbol{\kappa})^2 + m_Q^2} - \frac{\mathbf{l} - \boldsymbol{\kappa}}{(\mathbf{l} - \boldsymbol{\kappa})^2 + m_Q^2} + \frac{\mathbf{l} + \mathbf{q}/2}{(\mathbf{l} + \mathbf{q}/2)^2 + m_Q^2} + \frac{\mathbf{l} - \mathbf{q}/2}{(\mathbf{l} - \mathbf{q}/2)^2 + m_Q^2}, \end{aligned} \quad (2.5)$$

and we used

$$\mathbf{l} = \mathbf{k} + \left( z - \frac{1}{2} \right) \mathbf{q}, \quad M^2 = \frac{\mathbf{k}^2 + m_Q^2}{z(1-z)}. \quad (2.6)$$

The electronic decay width  $\Gamma(V \rightarrow e^+e^-)$  of the vector meson constrains the light-cone wave function. Explicitly, the decay constant  $g_V$  is

$$g_V = N_c \int \frac{dz d^2\mathbf{k}}{z(1-z)(2\pi)^3} \psi_V(z, \mathbf{k}) \frac{2}{3} M(M + m_Q), \quad (2.7)$$

it is related to the decay width through

$$\Gamma(V \rightarrow e^+e^-) = \frac{4\pi\alpha_{em}^2 e_Q^2}{3M_V^2} \cdot g_V^2. \quad (2.8)$$

In the present approach we assume real photons and therefore only transverse photon and vector-meson polarizations are taken into account. This is sufficiently good approximation for heavy-ion peripheral collisions where the nucleus charge form factor selects quasi-real photons.

The running scale of strong coupling constant for the evaluation of the two-gluon exchange cross section is taken as:

$$\mu^2 = \max\{\kappa^2, \mathbf{k}^2 + m_Q^2\}. \quad (2.9)$$

For the radial wave function we use a Gaussian parametrization

$$\psi_V(z, \mathbf{k}) = N \cdot \exp[-ap^2], \quad p^2 = \frac{1}{4} \left( \frac{\mathbf{k}^2 + m_Q^2}{z(1-z)} - 4m_Q^2 \right). \quad (2.10)$$

Where the constants  $N, a$  are determined from the decay width (2.7,2.8) and the normalization condition

$$N_c \cdot \int \frac{dz d^2 \mathbf{k}}{(2\pi)^3 z(1-z)} M^2 |\psi_V(z, \mathbf{k})|^2 = 1. \quad (2.11)$$

For the case of  $J/\psi$  of interest here, we use  $m_Q = m_c = 1.5 \text{ GeV}$  and  $a = 1.37 \text{ GeV}^{-2}$ . In this way we get a good description of the  $\gamma p \rightarrow J/\psi p$  experimental data [10].

### C. Non-relativistic limit

In previous calculations in the literature the extreme non-relativistic approximation appropriate for the weakly bound state of heavy quarks has been adopted. In this case any quantum motion in the bound state is neglected, and one uses effectively:

$$\psi_V(z, \mathbf{k}) = C \cdot \delta\left(z - \frac{1}{2}\right) \delta^{(2)}(\mathbf{k}). \quad (2.12)$$

Notice that this means that quark and antiquark momenta in the boosted bound state are collinear. The constant  $C$  results as

$$C = \frac{2\pi^3}{N_c M_V^2} \sqrt{\frac{3M_V}{\pi}} \cdot \mathcal{R}(0) = \frac{1}{e_Q \alpha_{em}} \frac{\pi^3}{N_c M_V} \sqrt{\frac{3M_V \Gamma(V \rightarrow e^+ e^-)}{\pi}}. \quad (2.13)$$

Furthermore, for the weakly bound state  $M_V = 2m_Q$ . In the impact factor, we can now approximate  $I(T, T) = m_Q^2 \Phi_2$ , and the structure  $\Phi_2$  simplifies to (hereafter NR means non-relativistic):

$$\Phi_2^{\text{NR}} = 2 \cdot \left\{ \frac{1}{\boldsymbol{\kappa}^2 + M_V^2/4} - \frac{4}{\mathbf{q}^2 + M_V^2} \right\}. \quad (2.14)$$

The impact factor thus becomes:

$$\mathcal{J}^{\text{NR}}(\gamma_\lambda \rightarrow V_\tau; \boldsymbol{\kappa}, \mathbf{q}) = \delta_{\lambda, \tau} \frac{\sqrt{N_c^2 - 1}}{N_c} \alpha_S \frac{M_V}{4} \sqrt{\frac{3M_V \Gamma(V \rightarrow e^+ e^-)}{\alpha_{em}}} \cdot \Phi_2^{\text{NR}}. \quad (2.15)$$

### D. Meson exchange processes

The  $J/\psi$  meson decays into a photon and pseudoscalar meson [7]. The corresponding partial decay width can be used to calculate corresponding coupling constant  $g_{\gamma M J/\psi}^2 \propto \Gamma_{J/\psi \rightarrow \gamma M(0^-)} / p_{dec}^3$ .

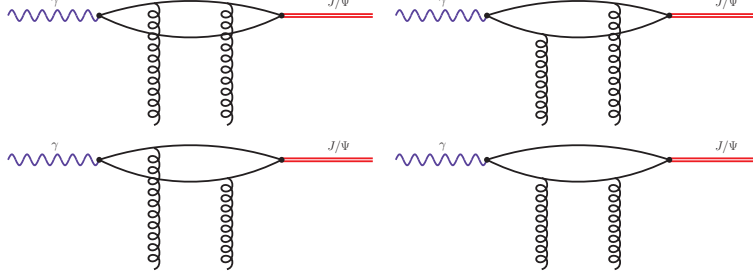


FIG. 4: Graphical representation of the two-gluon impact factor for the  $\gamma \rightarrow J/\psi$  transition.

The amplitude for the  $\gamma\gamma \rightarrow J/\psi J/\psi$  due to pseudoscalar meson ( $M$ ) exchange shown in Fig.3 can be written as:

$$\begin{aligned}
\mathcal{M}_{\lambda_1\lambda_2 \rightarrow \lambda_3\lambda_4}^M(k_1, k_2, p_1, p_2) &= g_{\gamma M J/\psi} \epsilon^{\mu_1\nu_1\alpha_1\beta_1} \epsilon_{\mu_1}(\lambda_1) \epsilon_{\nu_1}^*(\lambda_3) k_{1,\alpha_1} p_{1,\beta_1} \\
&\quad F_{\gamma M J/\psi}(t) \frac{-i}{t - m_M^2} F_{\gamma M J/\psi}(t) \\
&\quad g_{\gamma M J/\psi} \epsilon^{\mu_2\nu_2\alpha_2\beta_2} \epsilon_{\mu_2}(\lambda_2) \epsilon_{\nu_2}^*(\lambda_4) k_{2,\alpha_2} p_{2,\beta_2} \\
+ g_{\gamma M J/\psi} \epsilon^{\mu_1\nu_1\alpha_1\beta_1} \epsilon_{\mu_1}(\lambda_1) \epsilon_{\nu_1}^*(\lambda_4) k_{1,\alpha_1} p_{2,\beta_1} \\
&\quad F_{\gamma M J/\psi}(u) \frac{-i}{u - m_M^2} F_{\gamma M J/\psi}(u) \\
&\quad g_{\gamma M J/\psi} \epsilon^{\mu_2\nu_2\alpha_2\beta_2} \epsilon_{\mu_2}(\lambda_2) \epsilon_{\nu_2}^*(\lambda_3) k_{2,\alpha_2} p_{1,\beta_2} . \quad (2.16)
\end{aligned}$$

Above we add  $t$  and  $u$  meson exchange amplitudes. Compared to the  $J/\psi \rightarrow \gamma M$  decay in the  $\gamma\gamma \rightarrow J/\psi J/\psi$  process the exchanged mesons ( $M = \pi, \eta, \eta_c$ ) are off mass shell. This requires to introduce corresponding form factors ( $F$  in (2.16)). In the following they are parametrized in the exponential form as:

$$F(k^2) = \exp\left(\frac{k^2 - m_M^2}{2\Lambda^2}\right), \quad (2.17)$$

where  $k$  is four-momentum of the exchanged meson. We take  $\Lambda = 1$  GeV to estimate the meson exchange contributions. We have found that the cross section for the exchange of  $\pi^0$ ,  $\eta$  and  $\eta_c$  is very small, several orders of magnitude smaller than the cross section for the box and two-gluon exchange mechanisms. This is very different than for the production of pairs of light mesons in photon-photon scattering where the exchange of  $t$  or  $u$  channel mesons lead to relatively big cross section of the order of 1-10 nb.

The contributions of  $\pi$  and  $\eta$  meson exchange are small because corresponding coupling constants  $J/\psi$ -meson-photon are small compared to the case of  $\rho$  or  $\omega$  decays as can be deduced from the partial decay widths. The contribution of  $\eta_c$  exchange is suppressed by large  $\eta_c$  mass in the propagator.

### E. Equivalent Photon Approximation for $AA \rightarrow AA J/\psi J/\psi$

The total cross section can be calculated by the convolution:

$$\sigma(AA \rightarrow J/\psi J/\psi AA; s_{AA}) = \int dx_1 dx_2 \sigma(\gamma\gamma \rightarrow J/\psi J/\psi; x_1 x_2 s_{AA}) \frac{dn_{\gamma\gamma}(x_1, x_2, \mathbf{b})}{dx_1 dx_2} \quad (2.18)$$

The effective Weizsäcker–Williams photon fluxes can be calculated from:

$$dn_{\gamma\gamma}(x_1, x_2, \mathbf{b}) = \int d^2\mathbf{b}_1 d^2\mathbf{b}_2 \delta^{(2)}(\mathbf{b} - \mathbf{b}_1 + \mathbf{b}_2) S_{\text{abs}}^2(\mathbf{b}) \frac{1}{\pi} \frac{dx_1}{x_1} |\mathbf{E}(x_1, \mathbf{b}_1)|^2 \frac{1}{\pi} \frac{dx_2}{x_2} |\mathbf{E}(x_2, \mathbf{b}_2)|^2 \quad (2.19)$$

The presence of the absorption factor  $S_{\text{abs}}^2(\mathbf{b})$  assures that we consider only peripheral collisions, when the nuclei do not undergo nuclear breakup. Following [11] this can be taken into account as:

$$S_{\text{abs}}^2(\mathbf{b}) = \theta(\mathbf{b} - 2R_A) = \theta(|\mathbf{b}_1 - \mathbf{b}_2| - 2R_A) . \quad (2.20)$$

Thus in the present case, we concentrate on processes with final nuclei in the ground state. The electric fields can be expressed through the charge form factor of the nucleus:

$$\mathbf{E}(x, \mathbf{b}) = Z\sqrt{4\pi\alpha_{em}} \int \frac{d^2\mathbf{q}}{(2\pi^2)} e^{-i\mathbf{q}\mathbf{b}} \frac{\mathbf{q}}{\mathbf{q}^2 + x^2 M_A^2} F_{em}(\mathbf{q}^2 + x^2 M_A^2) . \quad (2.21)$$

Different forms of charge form factors are used in the literature. Here we use charge form factor calculated as a Fourier transform of the charge distribution. It was shown in Ref.[12, 13] to be crucial to take the realistic form factors.

### III. RESULTS

#### A. $\gamma\gamma \rightarrow J/\psi J/\psi$ reaction

Let us start from presenting our relativistic impact factors. In Fig.5 we show the forward ( $\mathbf{q}^2 = 0$ ) impact factor as a function of gluon transverse momentum squared.

One can observe a quick rise of the impact factor till gluon momentum transfer  $\kappa^2 \approx 3 \text{ GeV}^2$ . The impact factor obtained in the present relativistic approach (solid line) is much smaller than that obtained in the non-relativistic approach (dashed line) used in the literature. This will lead to corresponding differences in the amplitude of the  $\gamma\gamma \rightarrow J/\psi J/\psi$  process and related cross section.

Let us illustrate the situation for the amplitude. In Fig.6 we show rather integrands:  $dA/d\kappa$  (left panel) and  $dA/d\phi$  (right panel) instead of the whole amplitude. Here  $\phi$  is azimuthal angle between two-dimensional vectors  $\boldsymbol{\kappa}$  and  $\mathbf{q}$ . This figure demonstrates also that it is relatively easy to get numerical convergence of the integration in calculating the amplitude of the process, the decrease in  $\kappa$  is rather fast, the oscillation in  $\phi$  is relatively shallow.

In Fig.7 we show the dependence of the cross section on two-momentum transfer squared at energy  $\sqrt{s} \gg 2m_{J/\psi}$ . These two-gluon exchange distributions scale at larger energies. At smaller energies kinematical limitations due to energy-momentum conservation as well as interference of  $t$  and  $u$  diagrams due to identity of particles (two identical  $J/\psi$ 's) have to be included which destroys the scaling behavior. Fortunately both effects happen when



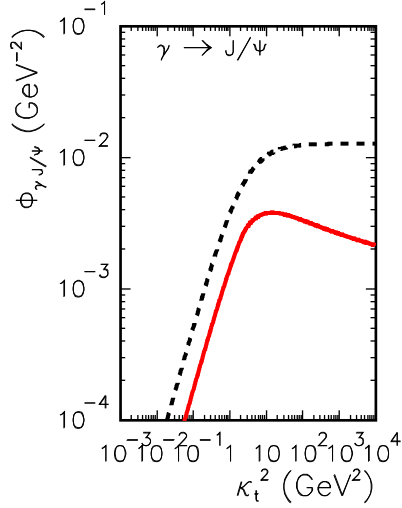


FIG. 5: Forward impact factor for  $\gamma \rightarrow J/\psi$  as a function of gluon momentum transfer squared. The solid line is our new result within the relativistic approach. Here  $\Phi_{J/\psi}(\kappa^2)\delta_{\lambda_1\lambda_3} = \mathcal{J}(\gamma_{\lambda_1} \rightarrow V_{\lambda_3}; \boldsymbol{\kappa}, \mathbf{q} = 0)$  (see Eq.(2.1)). For comparison we also show the impact factor in the non-relativistic approach (dashed line).

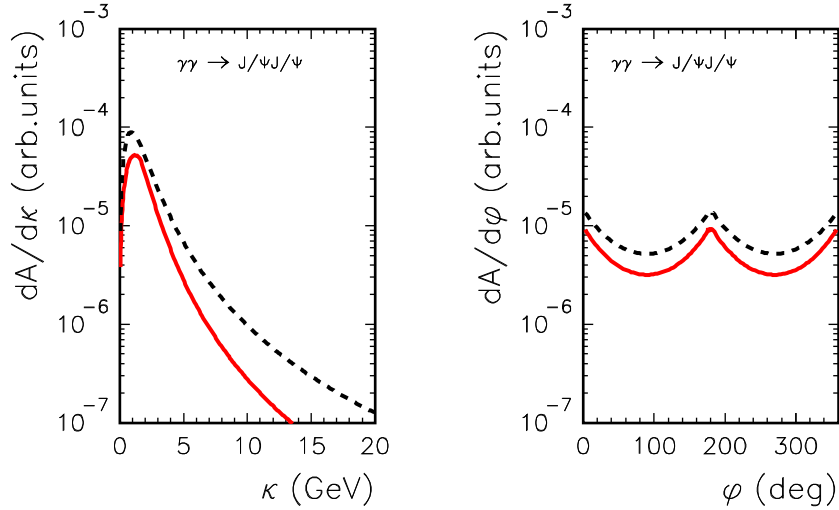


FIG. 6: Integrands of the amplitude as a function of  $\kappa$  for  $q_t^2 = 0$  (left panel) and as a function of  $\phi$  for  $q_t^2 = 5$  GeV (right panel). The solid line is our new result within the relativistic approach. For comparison we show results for the non-relativistic approach (dashed line).

$W < 10$  GeV, i.e. when the contribution of the two-gluon exchange is much smaller than that for the box mechanism as will be shown below. The power-like distribution shown in the figure strongly deviates from exponential dependence which was assumed for simplicity in previous calculations (see e.g. [3, 4]).

A brief discussion of the infrared sensitivity of the cross section is in order. Certainly, the

cross section is infrared safe – the impact factors vanish, when the transverse momenta of  $t$ -channel gluons go to zero. However this does not mean that there is no numerical sensitivity to the domain of small gluon transverse momenta, where the use of perturbation theory is not warranted. To investigate this sensitivity, we introduced a mass for the  $t$ -channel gluons. Notice that this mass does not affect the gauge invariance driven cancellation of impact factors which guarantee finiteness of the cross section.

Numerically, the infrared sensitivity is quite strong:

$$\frac{\sigma(\gamma\gamma \rightarrow J/\psi J/\psi; \mu_G = 0.7 \text{ GeV})}{\sigma(\gamma\gamma \rightarrow J/\psi J/\psi; \mu_G = 0 \text{ GeV})} \approx 0.45. \quad (3.1)$$

Here, the value  $\mu_G = 0.7 \text{ GeV}$  corresponds to a vacuum correlation length of gluons of  $R_c \sim 0.29 \text{ fm}$ . It is motivated by a number of phenomenological approaches to high-energy scattering [14, 15]. An analysis of gluon field-strength correlators on the lattice [16] also suggests a correlation length in this ballpark. Our observation of a surprisingly strong infrared sensitivity of the  $\gamma\gamma \rightarrow J/\psi J/\psi$  cross section agrees with Ref.[17], which uses the non-relativistic limit of the amplitude.

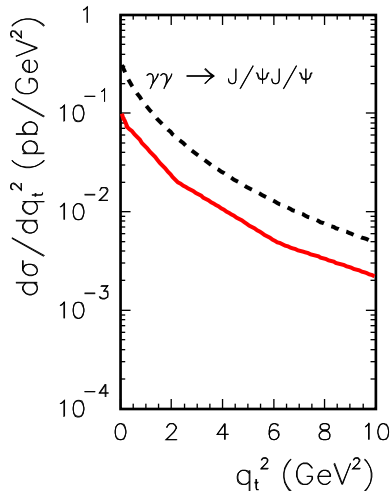


FIG. 7: Dependence of the  $\gamma\gamma \rightarrow J/\psi J/\psi$  cross section on momentum transfer squared. The solid line represents relativistic approach and the dashed line the non-relativistic approach.

The total cross section for the  $\gamma\gamma \rightarrow J/\psi J/\psi$  reaction is shown in Fig.8. We show separate contributions of the box diagrams (dashed line) as well as of the two-gluon exchange (dotted line). The second contribution scales at larger energy. Any higher-order interaction ( $t$ -channel ladder exchange) would increase the Born cross section. Unfortunately the existing calculation in the literature are limited to leading-order BFKL type of calculation [2, 3] which is known at present to strongly overestimate the cross section for other reactions. We leave a realistic evaluation of the increase of the cross section for future studies.

The box and two-gluon exchange cross sections have quite different energy dependence. As a consequence they are of similar size only in a very limited range of energy. Therefore in practice the interference effect can be neglected.

The suppression of the relativistic amplitude in comparison to its non-relativistic limit can be traced back to the suppression from the off-shell quark propagators in Eq.(2.5).

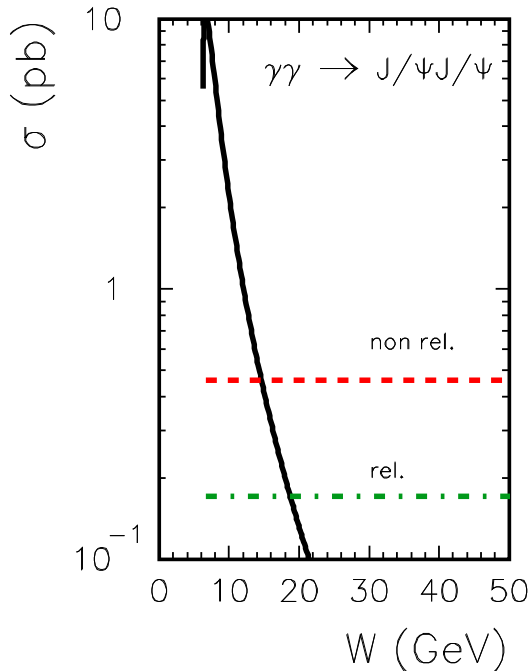


FIG. 8: Energy dependence of the  $\gamma\gamma \rightarrow J/\psi J/\psi$  cross section. The solid line is for the the box contribution (dashed line) while the dashed and dash-dotted lines for two-gluon exchange contribution in non-relativistic and relativistic approaches, respectively.

### B. $AA \rightarrow AJ/\psi J/\psi A$ reaction

Now we pass to the calculation of the cross section for nuclear collisions. We follow similar analyses for exclusive production of  $\rho^0\rho^0$  [12],  $\mu^+\mu^-$  [13],  $c\bar{c}$  [18] or  $\pi\pi$  [19]. In those approaches a calculation of the distribution in rapidity of the pair or invariant mass of the pair is particularly easy. In Fig.9 we show distribution in rapidity of the pair for  $W_{NN} = 2.76$  TeV. Both contributions (box and two-gluon exchange) are shown separately. The phase space integrated nuclear cross section is  $\sigma = 0.1 \mu\text{b}$ . which is of similar size as the cross section for production of  $D\bar{D}$  meson pairs [20]. The contribution of the two-gluon exchange is an order of magnitude smaller than that for the box mechanisms. No previous evaluation of the nuclear cross section included the dominant box contribution. In Fig.10 we show distribution in  $J/\psi J/\psi$  invariant mass. This distribution drops quickly as a function of the two-meson invariant mass, which reflects the fall-off of the effective photon-photon luminosity at large  $\gamma\gamma$ -energies. The two-gluon exchange contribution shows up only at  $M_{J/\psi J/\psi} > 15$  GeV. The situation can improve slightly if the rise of the  $\gamma\gamma$  cross section due to BFKL-type effects were included. We do not expect, however, that a realistic calculation including a BFKL-type ladder interaction between two  $c\bar{c}$  pairs would change our predictions significantly for invariant  $J/\psi J/\psi$  masses smaller than say 50 GeV.

Recently we have calculated the cross section for exclusive production of single  $J/\psi$  meson [21]. In Fig.11 we compare the cross section for the pair production (photon-photon fusion) with that for the production of a single  $J/\psi$  via the “photon-pomeron” mechanism.

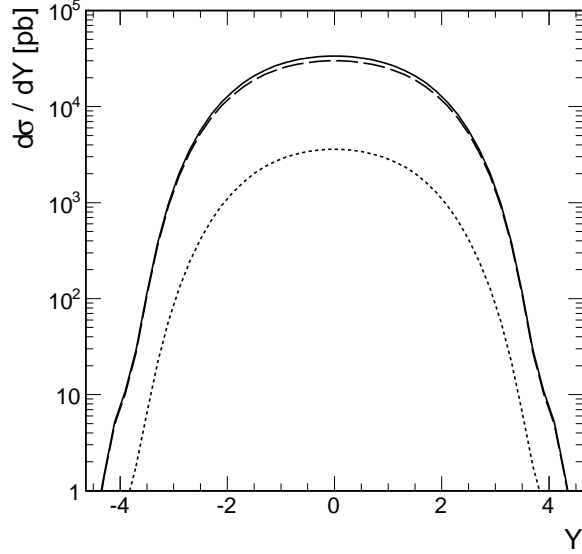


FIG. 9: Rapidity distribution of the  $J/\psi J/\psi$  pairs in  $^{208}\text{Pb} + ^{208}\text{Pb} \rightarrow ^{208}\text{Pb} + J/\psi J/\psi + ^{208}\text{Pb}$  process for  $W_{NN} = 2.76$  TeV. The dashed line is for the box contribution while the dotted line corresponds to the two-gluon exchange.

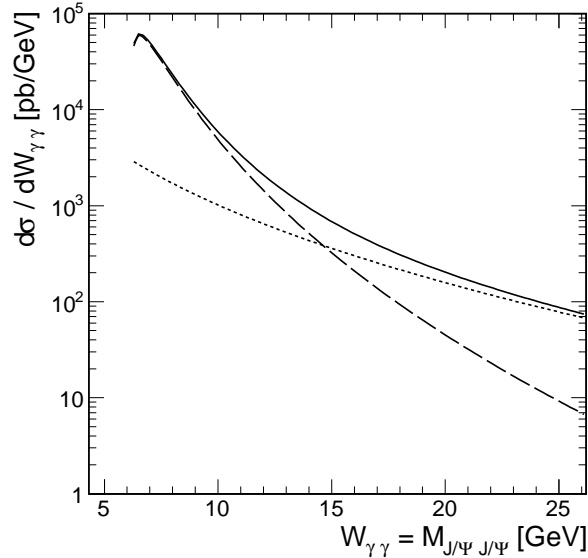


FIG. 10: Invariant mass  $J/\psi J/\psi$  pair distribution in  $^{208}\text{Pb} + ^{208}\text{Pb} \rightarrow ^{208}\text{Pb} + J/\psi J/\psi + ^{208}\text{Pb}$  process for  $W_{NN} = 2.76$  TeV. The meaning of the curves is the same as in the previous figure.

The latter cross section is more than five orders of magnitude larger. The single  $J/\psi$  production was measured e.g. at RHIC [22]. Similar analysis is being performed by the ALICE collaboration at the LHC [23]. A present statistics is a few hundreds of  $J/\psi$  [24]. This means that with present statistics the number of measured pairs would be less than one. Clearly a better statistics is necessary to see pairs of  $J/\psi$ . A better situation could

be for the  $pp \rightarrow ppJ/\psi J/\psi$  reaction where the effective  $\gamma\gamma$  luminosity at large  $J/\psi J/\psi$  invariant masses is much larger.

If the nuclear cross section for  $^{208}\text{Pb}+^{208}\text{Pb} \rightarrow ^{208}\text{Pb}(J/\psi J/\psi)^{208}\text{Pb}$  was much larger than predicted in this paper it could mean that a double scattering photon-pomeron mechanism discussed in Ref.[21] plays important role. A measurement of pair production at ALICE can therefore provide a quite new information. The exclusive nuclear double-scattering production of mesons was not discussed so far in the literature.

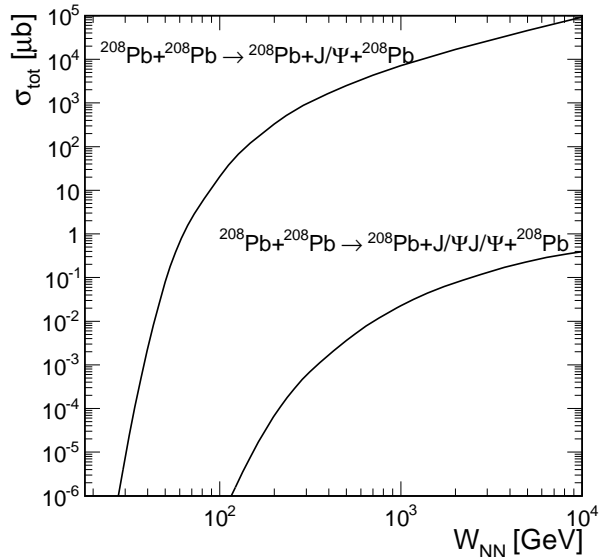


FIG. 11: Energy dependence of the cross section for the  $^{208}\text{Pb}+^{208}\text{Pb} \rightarrow ^{208}\text{Pb}+J/\psi J/\psi+^{208}\text{Pb}$  process versus that for the  $^{208}\text{Pb}+^{208}\text{Pb} \rightarrow ^{208}\text{Pb}+J/\psi+^{208}\text{Pb}$  process. The latter cross section is taken from [21].

#### IV. CONCLUSIONS

In the present paper we have calculated the total cross section and angular distributions for the  $\gamma\gamma \rightarrow J/\psi J/\psi$  process. For the first time we have included both formally two-loop contribution, called here “box contribution”, included so far in only one previous study, as well as two-gluon exchange contribution, formally higher order, discussed already in the literature. We have clarified a disagreement of results of different calculations in the literature. In our approach the two-gluon exchange contribution has been calculated in a relativistic approach with the wave function adjusted to reproduce the HERA data for  $\gamma p \rightarrow J/\psi p$  reaction. For the first time we have calculated relativistic off-forward two-gluon exchange amplitude. We have quantified a difference between the relativistic and non-relativistic approach used so far in the literature. The relativistic approach with “realistic” quark-antiquark  $J/\psi$  wave function gives smaller cross sections than those obtained in non-relativistic approximation. In addition, we have also estimated a contribution of pseudoscalar ( $\pi^0, \eta, \eta_c$ ) meson exchange mechanism. The latter ones turned out to be practically negligible.

The elementary cross section has been used to calculate cross section for ultra-peripheral ultra-relativistic heavy ion collisions ( $AA \rightarrow AJ/\psi J/\psi A$ ) at the LHC. In this context we have used equivalent photon approximation in the impact parameter representation and realistic charge form factor of the  $^{208}\text{Pb}$  nucleus. The nuclear cross section has been estimated and distribution in the  $J/\psi J/\psi$  rapidity and invariant mass have been presented. The cross section for double  $J/\psi$  production was compared with that for single  $J/\psi$  production from [21]. At the LHC energies the double  $J/\psi$  production cross section is smaller by more than five orders of magnitude compared to that for single  $J/\psi$  production. A measurement of the  $J/\psi J/\psi$  pair production may be then rather difficult as one has to take into account in addition a product of respective branching fractions for decays into lepton-antilepton pairs. On the other hand much bigger cross section could be a signal of double scattering “sequential” production of two single  $J/\psi$ ’s.

In the present analysis we have concentrated on the photon-photon mechanism of the  $J/\psi J/\psi$  pair production. Evidently similar mechanisms exist for gluon-gluon (sub)processes, leading to the inclusive production of  $J/\psi J/\psi$  pairs in proton-proton collisions. Such a production has been observed recently by the LHCb collaboration [25]. Only the box-type diagrams were included in corresponding calculations [26, 27]. The two-gluon exchange mechanism considered here may in principle compete with the double-parton production mechanism of the  $J/\psi J/\psi$  pairs discussed recently in [26, 27].

After we have performed the calculation presented here we have found a new preprint [28] where the production of two vector mesons is discussed. Some additional photon-exchange processes are considered. In the  $\gamma\gamma$  channel, the authors do not discuss the dominant box-mechanism. Also, nuclear charge form factors which are important at large  $\gamma\gamma$  energies [12, 13] are neglected.

### Acknowledgments

We are indebted to Christoph Mayer for a discussion of the ALICE measurement of the  $J/\psi$  meson. This paper was partially supported by the Polish Grants DEC-2011/01/B/ST2/04535 and N N202 236 640.

- 
- [1] I. F. Ginzburg, S. L. Panfil and V. G. Serbo, Nucl. Phys. B **296**, 569 (1988).
  - [2] J. Kwieciński and L. Motyka, Phys. Lett. **B438**, 203 (1998).
  - [3] V. P. Goncalves and W. K. Sauter, Eur. Phys. J. C **44**, 515 (2005) .
  - [4] V. P. Goncalves and M. V. T. Machado, Eur. Phys. J. C **49**, 675 (2007).
  - [5] C.-F. Qiao, Phys. Rev. D **64**, 077503 (2001).
  - [6] C. -H. Chang, Nucl. Phys. B **172**, 425 (1980); R. Baier and R. Rückl, Phys. Lett. B **102**, 364 (1981); E. L. Berger and D. L. Jones, Phys. Rev. D **23**, 1521 (1981).
  - [7] J. Beringer et al. (Particle Data Group), Phys. Rev. D **86**, 010001 (2012).
  - [8] J. A. M. Vermaseren, *Symbolic Manipulations with FORM* (Computer Algebra Nederland, Kruislaan, SJ Amsterdam, 1991, ISBN 90-74116-01-9).
  - [9] I. P. Ivanov, N. N. Nikolaev and A. A. Savin, Phys. Part. Nucl. **37**, 1 (2006).
  - [10] A. Cisek, *Exclusive processes with large rapidity gaps in the formalism of unintegrated gluon distributions*, (PhD thesis, The Henryk Niewodniczański Institute of Nuclear Physics, Polish Academy of Sciences, Kraków, 2012)

- [11] G. Baur and L. G. Ferreira Filho, Nucl. Phys. A **518**, 786 (1990); R. N. Cahn and J. D. Jackson, Phys. Rev. D **42**, 3690 (1990).
- [12] M. Klusek, W. Schäfer and A. Szczurek, Phys. Lett. **B674** 92, (2009).
- [13] M. Klusek-Gawenda and A. Szczurek, Phys. Rev. **C82** 014904, (2010).
- [14] N. N. Nikolaev, B. G. Zakharov and V. R. Zoller, JETP Lett. **59**, 6 (1994); N. N. Nikolaev, B. G. Zakharov and V. R. Zoller, JETP Lett. **66**, 138 (1997) [Pisma Zh. Eksp. Teor. Fiz. **66**, 134 (1997)]; N. N. Nikolaev, W. Schäfer, B. G. Zakharov and V. R. Zoller, JETP Lett. **84**, 537 (2007).
- [15] B. Z. Kopeliovich, I. K. Potashnikova, B. Povh and I. Schmidt, Phys. Rev. D **76**, 094020 (2007).
- [16] M. D’Elia, A. Di Giacomo and E. Meggiolaro, Phys. Lett. B **408**, 315 (1997).
- [17] M. B. Gay Ducati and W. K. Sauter, Phys. Lett. B **521**, 259 (2001).
- [18] M. Klusek-Gawenda, A. Szczurek, M. Machado and V. Serbo, Phys. Rev. **C83** 024903, (2011).
- [19] M. Klusek-Gawenda and A. Szczurek, Phys. Lett. **B700** 322, (2011).
- [20] M. Luszczak and A. Szczurek, Phys. Lett. **B700** 116, (2011).
- [21] A. Cisek, W. Schäfer and A. Szczurek, Phys. Rev. C **86**, 014905 (2012).
- [22] S. Afanasiev et al. (PHENIX Collaboration), Phys. Lett. **B679** 321, (2009).
- [23] A. Nystrand, a talk at the Blois workshop, Qui Nhon, Vietnam, December 2011.
- [24] Ch. Mayer, *private communication*, July 2012.
- [25] R. Aaij et al. (LHCb collaboration), Phys. Lett. **B707** 52, (2012).
- [26] C.H. Kom, A. Kulesza and W.J. Stirling, Phys. Rev. Lett. **107** 082002, (2011).
- [27] S.P. Baranov, A.M. Snigirev and N.P. Zotov, Phys. Lett. **B705** 116, (2011).
- [28] A. I. Ahmadov, B. A. Kniehl, E. A. Kuraev and E. S. Scherbakova, arXiv:1206.4441 [hep-ph].